Published in final edited form as:
Circ Res. 2010 March 19; 106(5): 971–980. doi:10.1161/CIRCRESAHA.109.210682.

Relative Roles of Direct Regeneration Versus Paracrine Effects of Human Cardiosphere-Derived Cells Transplanted Into Infarcted Mice

Isotta Chimenti, **Rachel Ruckdeschel Smith**, **Tao-Sheng Li**, **Gary Gerstenblith**, **Elisa Messina**, **Alessandro Giacomello**, and **Eduardo Marbán**

Department of Experimental Medicine (I.C., E. Messina, A.G.), Pasteur Institute, Cenci Bolognetti Foundation, "Sapienza" University of Rome, Italy; Cedars-Sinai Heart Institute (R.R.S., T.-S.L., E. Marbán), Los Angeles, Calif; and Division of Cardiology (G.G.), Johns Hopkins University, Baltimore, Md

Abstract

Rationale—Multiple biological mechanisms contribute to the efficacy of cardiac cell therapy. Most prominent among these are direct heart muscle and blood vessel regeneration from transplanted cells, as opposed to paracrine enhancement of tissue preservation and/or recruitment of endogenous repair.

Objective—Human cardiac progenitor cells, cultured as cardiospheres (CSps) or as CSp-derived cells (CDCs), have been shown to be capable of direct cardiac regeneration in vivo. Here we characterized paracrine effects in CDC transplantation and investigated their relative importance versus direct differentiation of surviving transplanted cells.

Methods and Results—In vitro, many growth factors were found in media conditioned by human adult CSps and CDCs; CDC-conditioned media exerted antiapoptotic effects on neonatal rat ventricular myocytes, and proangiogenic effects on human umbilical vein endothelial cells. In vivo, human CDCs secreted vascular endothelial growth factor, hepatocyte growth factor, and insulin-like growth factor 1 when transplanted into the same SCID mouse model of acute myocardial infarction where they were previously shown to improve function and to produce tissue regeneration. Injection of CDCs in the peri-infarct zone increased the expression of Akt, decreased apoptotic rate and caspase 3 level, and increased capillary density, indicating overall higher tissue resilience. Based on the number of human-specific cells relative to overall increases in capillary density and myocardial viability, direct differentiation quantitatively accounted for 20% to 50% of the observed effects.

Correspondence to E. Marbán, MD, PhD, Cedars-Sinai Heart Institute, 8700 Beverly Blvd, Los Angeles, CA 90048. eduardo.marban@csmc.edu.

Disclosures

Capricor Inc: E. Marbán (stock ownership), A.G. (consulting income), and R.R.S. (employment). No research support was provided by Capricor.

This manuscript was sent to David Eisner, Consulting Editor, for review by expert referees, editorial decision, and final disposition.

Conclusions—Together with their spontaneous commitment to cardiac and angiogenic differentiation, transplanted CDCs serve as "role models," recruiting endogenous regeneration and improving tissue resistance to ischemic stress. The contribution of the role model effect rivals or exceeds that of direct regeneration.

Keywords

paracrine hypothesis; cardiac stem cells; VEGF; HGF; IGF1

Cardiac cell therapy represents a major new frontier in heart disease treatment,[1-3] but the basic biological mechanisms underlying the reported beneficial effects remain poorly-characterized.[4 - 6] Cardiac and vascular differentiation of transplanted cells is only one of multiple pathways playing a role in the positive outcome of stem cell transplantation. An alternative explanation is the so called "paracrine hypothesis," which states that the release of cytokines and growth factors (GFs) by transplanted cells has a positive "bystander" effect on viability and recovery of the ischemic host tissue.[7-11] In fact, many benefits of cardiac cell therapy could be related, at least in part, to the ability of transplanted cells to secrete signaling molecules, which may influence cardiomyocyte survival, neoangiogenesis and/or possibly the recruitment of endogenous cardiac stem cells.[12]

The cardiac progenitor cell population used in the present study is isolated from explant cultures of adult human endomyocardial biopsies using an intermediate cardiosphere (CSp) step.[13,14] CSps are self-assembling spherical clusters that grow in semisuspension culture on poly-D-lysine, and that constitute a niche-like environment: undifferentiated cells proliferate in the core, whereas cardiac-committed cells grow on the periphery in a gradient fashion. CSp-derived cells (CDCs) can be expanded many fold as monolayers on fibronectin, achieving cell numbers suitable for cell therapy. CDCs have been shown[14] to improve left ventricular ejection fraction (LVEF) in SCID beige mice 3 weeks after acute myocardial infarction (MI), when compared to mice injected with vehicle or with adult normal human dermal fibroblasts (NHDFs). The clonogenicity and multilineage potential of CDCs have recently been confirmed, along with demonstration that the cells reflect neither cardiomyocyte remnants nor blood-borne contaminants.[15]

Our previous work on CDCs, and that of others,[16,17] supports the notion that such cells can directly regenerate myocardium and blood vessels.[14] In the present study, we investigated the hypothesis that paracrine mechanisms may also contribute to the beneficial effects of human CDCs. In vitro screening of conditioned media (CM) focused our study on three GFs, vascular endothelial growth factor (VEGF), hepatocyte growth factor (HGF), and insulin-like growth factor (IGF)-1, that have been shown to play important roles after MI,[18-24] including reducing cell death, improving microcirculation and partially preventing remodeling. The relevance of these factors has been recently investigated in multiple cardiac cell therapy settings.[7,9,25-30] We assessed whether CSps and CDCs release these GFs in vitro and whether they mediate the favorable biological effects of CDC-conditioned media (CDC-CM) on neonatal rat ventricular myocytes (NRVMs) and human umbilical vein endothelial cells (HUVECs). We also investigated the release of GFs in vivo by CDCs in infarcted SCID mice, and parameters such as the expression of survival markers, apoptotic

rate and capillary density in heart tissue at different time points. Finally we quantified the relative magnitudes of direct CDC differentiation and indirect paracrine effects. Our results support the notion that paracrine/humoral mechanisms play a major role in the overall beneficial effect of CDC treatment in the MI setting. This is the first report of quantification of direct and paracrine effects exerted by a cardiac resident progenitor population on cardiac tissue preservation and angiogenesis.

Methods

Cell Culture and Conditioned Media Collection

Human CSps and CDCs were obtained, as previously described,[14] from percutaneous septal endomyocardial biopsies from 21 different patients (Figure 1a), during clinically indicated procedures after informed consent, in an institutional review board–approved protocol.

Media were conditioned for 48 hours, and were either 2.5% FBS complete explant medium (CEM), or glucose-free FBS-free basal medium (BM). See the expanded Methods section (Online Data Supplement, available at http://circres.ahajournals.org) for detailed media recipes, as well as for protocols on protein array, ELISA, luciferase-lentivirus creation and transduction.

NRVM Culture and FACS Analysis

NRVMs were isolated as described.[31] Plates were incubated in humidified 2% O_2 atmosphere for 24 or 72 hours with CM or FBS-free BM (Figure 1b). Cells were then collected by trypsinization, labeled with Annexin V-FITC and 7AAD (BD Biosciences), and analyzed with a FACScan flow cytometer and CellQuest software (BD Biosciences).

Angiogenesis Assay

HUVECs were plated on precast, matrix-coated 96-well plates (BD Biosciences). They were plated either with endothelial cell media (Lonza), as positive control, or with CM (Figure 1b), or with FBS-free BM, as the negative control. Cells were imaged after 18 hours to reconstruct the complete image of every well (Online Figure I). The total tube length was then measured with the ImageJ plug-in, NeuronJ (NIH) (http://rsb.info.nih.gov/ij).

Mouse Myocardial Infarction Model

SCID beige mice (10 weeks old) were subjected to LAD ligation as previously described,[14] and 1×10^5 CDCs or NHDFs were acutely injected into the infarct border zone. Regional tissue samples were taken from infarct, border zone (BZ), right ventricle, and septum areas for Western blot (WB) and RT-PCR analysis (Figure 1b). For sectioning, hearts were arrested in diastole, fixed in formalin and paraffin embedded. At least 3 animals per group were considered for each experimental setting. See the expanded Methods section (Online Data Supplement) for details regarding tissue sectioning, immunofluorescence, protein and RNA extraction, WB, and PCR.

LVEF was calculated with VisualSonics version 1.3.8 software from 2D long-axis views taken through the infarcted area. Optical imaging was performed in the IVIS SPECTRUM

(Xenogen) imaging chamber. See the expanded Methods section (Online Data Supplement) for more details.

Statistical Analysis

All results are presented as mean value±standard deviation, unless specified. Significance of difference between any two groups was determined by two-sided Student *t* test. A final value of $P<0.05$ was considered significant.

Results

Preliminary Protein Array Screening

Serum-free CMs from CSps and CDCs were screened for secreted factors using a protein array. We sought to identify factors that were present in both cell products but enhanced in CSps, which have properties reminiscent of stem cell niches and potent regenerative bioactivity.[13,15] All 79 spots corresponding to various cytokines and growth factors gave a positive signal, despite variability in signal intensities. Figure 2 shows two representative blots from CSps and CDCs derived from the same patient sample, together with the corresponding densitogram, showing the CSp/CDC optical density ratios for each factor. Among the factors which showed several-fold enhancement in CSp-CM, we selected 3 candidates for further analysis, VEGF, HGF, and IGF1, based on the following criteria: (1) identity as nonimmunomodulatory factors; (2) high CSp/CDC ratio, reporting the ability to enhance secretion in 3D culture; and (3) well-known roles in cardiac pathophysiology, in particular in MI and heart failure.[7-9,18-30]

CSps, CDCs, and Secondary Cardiospheres Release GFs In Vitro

One goal was to compare the paracrine potencies of three potential cell delivery products: CSps, CDCs, and secondary CSps that were rederived from passaged CDCs (IICSps). Analysis of low-serum CM revealed that CSps, CDCs and IICSps secrete significant amounts of GFs in culture (Figure 3a). During 48 hours of conditioning in low serum, CSps released VEGF, HGF, and IGF1. By contrast, in the same culture conditions, CDCs and IICSps released only VEGF in measurable amounts, although secretion by IICSps was at the level measured in CSps. Different culture settings were examined (different serum concentrations and multiple cell densities), but IGF1 secretion was never detected again after the CSp stage (data not shown). Nevertheless, CDCs can release HGF in vitro under certain conditions, as detected by ELISA in BM (Figure 3b). Immunofluorescent analysis of CSps revealed ample VEGF, HGF, and IGF1 (Figure 3c and 3d). Reverse transcription PCR on RNA isolated from CSps, CDCs and IICSps confirmed the expression of VEGF, HGF, and IGF1 mRNAs at all stages (Figure 3e). No GFs were detected by ELISA in NHDF-CM in any of the conditions tested, although we could detect the expression of the corresponding mRNAs by PCR. NHDFs were also grown as spheres on poly-D-lysine, but we could detect neither cell-associated GFs by immunofluorescence (data not shown) nor secreted GFs in CM by ELISA (Figure 3a).

CSps and CDCs also express the receptors for VEGF, HGF, and IGF1 (respectively KDR, Met, IGF1-R), as assessed by immunofluorescence and RT-PCR (Online Figure II).

Effect of CDC-CM on NRVM Viability

CDC- and NHDF-CM were collected in FBS-free BM and used to replace NRVM media. After 24 or 72 hours in 2% hypoxia, the percentage of early apoptotic NRVMs was assessed by AnnexinV/7AAD labeling. Whereas no differences were apparent at 24 hours, after 72 hours the percentage of early apoptotic NRVMs was dramatically lower in the CDC-CM (Figure 4a) compared to the NHDF-CM (Figure 4b) and the control FBS-free BM (Figure 4c and 4d). This effect was partially but significantly reduced when NRVMs were plated for 72 hours with CDC-CM that had been preincubated with both neutralizing anti-VEGF and HGF antibodies (Figure 4e). The neutralization of both secreted GFs resulted in an excess 23% early apoptotic NRVMs compared to plain CDC-CM. The neutralizing antibodies were not degraded and were still detectable by WB in the media after 72 hours of culture (Online Figure III).

Effect of CDC-CM on HUVEC Angiogenic Properties In Vitro

CDC transplantation induces both cardiomyogenesis and angiogenesis.[14] To investigate the effects of CM on blood vessel formation, HUVECs were subjected to an in vitro angiogenesis assay in endothelial cell media (Figure 4f), FBS-free BM (Figure 4g) or CM (Figure 4h and 4i). The ability of HUVECs to form complex tube networks was lost in BM, but in the presence of CDC-CM this ability was almost completely recovered (Figure 4h). This effect was also dramatically greater than that seen with NHDF-CM (Figure 4i and 4j). Preincubation with anti-VEGF or both anti-VEGF and anti-HGF neutralizing antibodies caused a slight but significant reduction of the total tube length per well (Figure 4k).

CDCs Release GFs In Vivo

We took advantage of human-specific sequences and epitopes (Online Figure IV) to detect factors secreted by human cells transplanted into injured mouse hearts. SCID mice were subjected to LAD ligation and injected with 10^5 CDCs or NHDFs. One day and 1 week after cell delivery, VEGF, HGF, and IGF1 human mRNAs were detectable in the infarct area of CDC- and NHDF-injected mice (Figure 5a). Despite that, we could detect human GFs by WB with human-specific antibodies only in CDC-injected animals, although hGAPDH was evident in the infarct and BZ of both CDC- and NHDF-injected animals (Figure 5b), indicating survival of the cells for three weeks in CDC-injected and for at least 1 week in NHDF-injected hearts. GFs were also detectable in remote areas, like the right ventricle and septum, 1 day after cell delivery. After 3 weeks bands for hHGF and hIGF1 were faint, but detectable, although hVEGF could no longer be found; nevertheless, CDCs had engrafted and survived in the infarct and border zones, as evidenced by the detection of hGAPDH in tissue lysates by WB (Figure 5b) and by immunodetection of human cells in tissue sections (data not shown; also previously[14]).

The absence in the WB of a hGAPDH band in the BZ after 24 hours can be attributed, at least in part, to the difficulty in distinguishing the infarct from the peri-infarct zone at such an early time point.

CDC-Injected Heart Tissue Displays Higher Tissue Viability and Capillary Density

The 1 week time point was chosen as an optimal time to examine tissue viability and capillary density. One week after cell delivery, GF levels remain high in the heart (Figure 5), and a strong trend toward a higher LVEF is already noticeable in the CDC group compared to the NHDF control (Figure 6a). Lysates from CDC-injected mice contained higher levels of Akt protein compared to NHDF-injected animals, as shown by WB and relative densitometric analysis (Figure 7a). Moreover, active Csp3 expression was reduced in CDC-injected hearts relative to controls. These results correlate with a reduced apoptotic rate (Figure 7b) and higher capillary density in the border zone of CDC-injected mice (Figure 7c), compared to controls, as assessed by TUNEL and isolectin B4 staining, respectively. Taken together, these data indicate that CDCs suppress postischemic apoptosis and improve blood supply.

Engraftment Levels and Paracrine Contribution

To begin to assess the relative roles of direct differentiation versus paracrine effects, we measured bioluminescence in mice that had been injected with luciferase-labeled CDCs. This method of detecting residual engraftment over time, although limited by factors such as signal attenuation by chest wall tissue and possible gene silencing, offers at least a qualitative sense of transplanted cell survival. Figure 6b shows that, after 1 week, the luciferase signal has already dropped to approximately 30% of that on day 1, and by week 3, cells are no longer detectable using this technique. Similarly low survival at 3 weeks has been previously reported with injected CDCs.[32,33] Despite this, the overall functional improvement in the CDC-treated group persists 3 weeks post-MI (Figure 6a), confirming previous findings.[14] Taken at face value, the bioluminescence data suggest that surviving CDCs are entirely irrelevant; however, the method is nonquantitative, because it is susceptible to tissue attenuation and reporter gene silencing.[34]

As a means of quantifying how much of the improvement is attributable to direct regeneration versus indirect humoral effects, we calculated the relative contribution of human CDCs to the capillary density in the tissue areas where CDCs were detectable after 1 week. Despite an overall doubling of capillary density in CDC-injected mice, only 9.6±2.7% of the total capillaries were found to be of human origin (Figure 8a). This amounts to ≈20% of the enhanced angiogenesis; thus, the angiogenic effect reflects both direct differentiation and paracrine effects, but the latter predominates. We next examined the cardiomyogenic effect of CDC transplantation. Consistent with our previous results at 3 weeks,[14] at 1 week the infarct area of CDC-injected mice contained a higher percentage of viable myocardium (Online Figure V), as assessed by Masson's trichrome staining. Within those viable areas, 11.8±4.5% of the myosin heavy chain (MHC)-expressing cells were of human origin (Figure 8b). This number, although significant, explains only half of the ≈20% increase in relative tissue viability revealed by Masson's trichrome staining, and only ≈25% of the overall doubling in MHC^+ nuclei (Figure 8b). Thus, both direct regeneration and paracrine effects underlie the cardiomyogenic effects of CDC transplantation. No human capillaries or MHC-positive cells were detectable in the NHDF-injected hearts.

If transplanted CDCs were acting to recruit endogenous repair, one might expect to observe an enrichment of endogenous progenitor cells in the vicinity of surviving CDCs. We have thus looked for colocalization of human CDCs with endogenous c-kit$^+$ or nkx2.5$^+$ cells. Foci of nonhuman c-kit$^+$ cells surrounding injected CDCs are clearly detectable 2 days after cell delivery, with some persistence 1 week (Online Figure VI, a). Likewise, nkx2.5$^+$ cells accumulate in the infarct area of CDC-injected mice at 1 week after cell delivery, with the proportion of nkx2.5$^+$ nuclei being significantly higher than in NHDF-injected controls (Online Figure VI, b). These data are consistent with the idea that transplantation of human CDCs recruits endogenous regeneration as part of the salutary mechanism.

Discussion

Because the administration of human CDCs improves cardiac function in a SCID mouse MI model,[14] we investigated the release of relevant GFs (VEGF, HGF, and IGF1) by human CSps and CDCs, and the potential contribution of paracrine mechanisms to the beneficial and protective effects of CDC-CM in vitro and of CDC therapy in vivo.

Preliminary screening of human CSp- and CDC-CM revealed that these populations are capable of releasing many different cytokines and growth factors, and provides leading information for future experiments (Figure 2). In the present study, though, we selected VEGF, HGF, and IGF1 as our main candidates for more extensive functional studies.

CSps spontaneously release significant and higher amounts of VEGF, HGF, and IGF1 in vitro than do CDCs, as assessed by ELISA. CDCs secrete only VEGF and HGF, although they maintain the transcription of all their mRNAs (Figure 3). On the other hand, IICSps were able to secrete VEGF at levels comparable to primary CSps, suggesting that at least for this GF the 3D structure might be a key factor influencing its release, possibly because of internal hypoxic stimulation.[35] These results suggest that: (1) the primary CSp is the stage at which paracrine abilities are maximal in vitro; (2) VEGF release is affected by the 3D structure; and (3) HGF and IGF1 release fades with progressive time in culture.

Interestingly, the absolute GF concentrations measured were approximately between 50 and 2000pg/mL, which correspond to the actual range of their circulating concentrations in physiological up to pathological conditions.[36-38] Furthermore, the expression of these GF receptors in CSps and CDCs (Online Figure II) suggests a possible autocrine feedback effect.

Although our results demonstrate that CSps are more potent in vitro, as far as VEGF, HGF, and IGF1 secretion is concerned, the expansion of progenitor cells as CDCs has proven to be closer to clinical translation (in the ongoing CADUCEUS trial; see http://clinicaltrials.gov for details), because coronary delivery can be safely performed with CDCs.[39] Therefore we have tested the biological effects of CDC-CM and shown for the first time a direct connection between the presence in the media of an active GF secreted by progenitor cells and a functional benefit in vitro. CDC-CM reduces the percentage of early apoptotic NRVMs in vitro (Figure 4a through 4e); this prosurvival effect is partially attributable to secreted VEGF and HGF in a synergistic way, as shown by the reduction of NRVM viability

after preincubation of the CDC-CM with both anti-VEGF and HGF neutralizing antibodies (Figure 4e). CDC-CM also has proangiogenic effects. In fact CDC-CM recovered almost completely the ability of HUVECs to form complex tube networks, which was lost in the unconditioned BM (Figure 4f through 4k). Again, VEGF secreted by CDCs plays an important role in the global effect, as demonstrated by the neutralizing antibody experiments, which showed a significant reduction in the enhanced tube formation.

We also tested whether CDCs can release GFs in vivo in the same murine MI model where they have been previously shown to improve LV function 3 weeks after MI,[14] a functional benefit confirmed here (Figure 6a). When acutely injected intramyocardially in infarcted SCID mice, CDCs release VEGF, HGF, and IGF1, detectable for at least 1 week after cell delivery by RT-PCR and WB with human specific primers and antibodies (Figure 5). Despite the fact that in both cell-treated groups human cells had engrafted, as shown by hGAPDH expression, GFs secreted by transplanted cells were detectable only in CDC-injected animals, ie, in the only group shown to achieve a significant functional improvement. The distribution of human GFs in remote areas (right ventricle, septum) 24 hours after cell injection might be attributable to diffusion via a relatively intact vascular system at that time, which was no longer functional in the more mature infarct scar 1 week after surgery, thus restraining human GFs around the CDC engraftment zone. Alternatively, the early spread into neighboring areas may simply reflect a greater intensity of GF production soon after injection, also resulting from the presence of many more cells.

Cell survival, particularly in an unfavorable environment (such as ischemic cardiac tissue), mostly depends on the ability of the cell to overcome death triggers and secondarily to promote angiogenesis. In this respect, the in vitro antiapoptotic and proangiogenic effects of CDC-CM correlate with the in vivo observation that, 1 week after cell delivery, Akt was upregulated in tissue samples from CDC-injected animals. Contemporaneously, the active form of the apoptotic effector Csp3 was less expressed in CDC- compared to NHDF-injected hearts (Figure 7a). Furthermore, the rate of TUNEL-positive cells was significantly reduced in the border zone of CDC-injected mice, which also displayed higher capillary density compared to controls (Figure 7b and 7c). Overall, our results imply that the injection of CDCs in infarcted SCID mouse hearts favors higher tissue viability in the infarct and peri-infarct areas, and consistently correlates with reduced apoptosis and improved blood supply. This notion is coherent with previous histological data showing a higher percentage of viable myocardium in the infarct area of CDC-injected, as compared to NHDF-injected mice,[14] confirmed at the 1 week time point in the present study (Online Figure V).

Human CDCs and/or their progeny persist for at least three weeks, as gauged by the robust hGAPDH protein signal, whereas NHDFs disappear sometime between 1 and 3 weeks. It is not yet clear whether the persistence of CDCs reflects their multilineage differentiation,[14] a survival advantage conferred by paracrine effects such as those described here, or a combination of both mechanisms. Accordingly, we also attempted a quantitative evaluation of the balance between direct and indirect beneficial effects in CDC therapy (Figure 8). The quantification of human nuclear antigen (HNA)-positive capillaries in the border zone indicates that, after one week, CDCs directly contribute to approximately 10% of the overall capillary density in the areas of CDC engraftment. Even if this fraction is subtracted, there is

still a statistically significant difference between the CDC and the NHDF groups, confirming the major role of indirect paracrine induction by CDCs.

To evaluate direct contributions to cardiomyogenesis in the areas of engraftment, we quantified the fraction of HNA/MHC double-positive cells in the viable areas of myocardium in the infarct of CDC-injected mice at 1 week (Figure 8b). Approximately 12% of the MHC-positive cells were also HNA-positive, and this fraction was necessary to reach statistical significance versus the NHDF group, therefore suggesting at least parity between direct and indirect mechanisms.

It is important to point out that paracrine effects might include two distinct phenomena: the first is humoral stimulation of endogenous regeneration, and the second is preservation of preexisting cells. Although we suspect that both are operative, our results do not enable us to conclusively dissect the relative roles of recruitment versus enhanced tissue survival attributable to the demonstrated antiapoptotic effects of CDCs. Direct injection of HGF and IGF1 into the myocardium has been shown to successfully mobilize endogenous cardiac stem cells[40]; given that CDC transplantation produces these same GFs, involvement of endogenous stem cells is very likely to contribute to the functional improvement, as also suggested by colocalization of injected CDCs with endogenous c-kit$^+$ and nkx2.5$^+$ cells (Online Figure VI).

Given that long-term engraftment of transplanted cells is low and that the final benefit reflects both direct and indirect effects, it seems reasonable to focus on enhancing engraftment and paracrine potency, as prime strategies to boost the overall efficacy of cell therapy.

The potential use of cytokines and GFs as cardiac therapeutic tools has been carefully investigated in the past few years, especially by means of gene therapy. Although interesting results have been obtained in preclinical and early clinical studies on proangiogenic treatments for heart failure and coronary disease, unfortunately these protocols involve risks such as pathological angiogenesis, severe inflammatory reactions and arrhythmias.[41,42] The possibility of a GF release under biological and physiological control through stem cell therapy might offer an ideal combination of strategies.[43] In this respect, an attractive constellation in therapeutic candidates is the dual ability of cardiac progenitor cells to differentiate directly, but also to secrete beneficial molecules and harness tissue preservation and/or endogenous repair. In vitro and in vivo results on cytoprotective effects on cardiomyocytes and on enhanced neovascularization, similar to the ones presented here, have been reported by mesenchymal stem cells, bone-marrow mononuclear cells and endothelial progenitor cells (see elsewhere[12] for a complete review). This, however, is the first report assessing in detail the role and proportion of paracrine effects mediated by a resident cardiac progenitor population.

In conclusion, CSps and CDCs secrete significant amounts of prosurvival and proangiogenic GFs in vitro, and CDCs are able to secrete VEGF, HGF, and IGF1 in a murine cardiac cell therapy model as well. This appears to be a key mechanism, together with their natural

propensity for cardiac differentiation, contributing to their regenerative potential and therapeutic effects in the postinfarction period.

EXPANDED MATERIALS AND METHODS

Cell culture and conditioned media collection

Human CSps and CDCs were obtained, as previously described[1], from percutaneous septal endomyocardial biopsies from 21 different patients, during clinically indicated procedures after informed consent, in an institutional review board-approved protocol. CSps were grown on poly-D-Lysine (BD Biosciences) coated plates in CSp growth medium (CGM): 35% IMDM and 65% DMEM/F-12 Mix, 3.5% FBS (Hyclone), 1% penicillin-streptomycin, 1% L-glutamine, 0.1mmol/L 2-mercaptoethanol, 1 unit/mL thrombin (Sigma), 1:50 B-27 (Invitrogen), 80ng/mL bFGF, 25ng/mL EGF and 4ng/mL cardiotrophin-1 (Peprotech). CDCs and NHDFs were grown in 20% FBS complete explant medium (CEM): IMDM, 1% penicillin-streptomycin, 1% L-glutamine, 0.1mM 2-mercaptoethanol. CDCs were cultured on FN (Sigma) coated flasks. Cells were used for all experiments between the first and forth harvest from the explant, and between passage 1 and passage 3 on FN. Secondary CSps (IICSps) or NHDF-spheres were obtained by plating CDCs or NHDFs, respectively, in CGM on poly-D-lysine coated multiwells (fig.1a) at a density of 1×10^4 cells/cm^2. Media were conditioned for 48 hours by CSps and IICSps after 4-5 days of culture on poly-D-Lysine, or by CDCs and NHDFs when they were approximately 90% confluent. Media for conditioning were 2.5% FBS CEM, or glucose-free FBS-free basal medium (BM): Medium 199, 10mmol/L HEPES, 0.1mmol/L MEM non-essential amino acids, 2mmol/L L-glutamine, 0.8μg/mL vitamin B12, 2 unit/mL penicillin. CMs were stored at −80°C until used. In some experiments CMs were pre-incubated on a shaker for 1 hour at room temperature with anti-VEGF (R&D System) and/or anti-HGF (Abcam) neutralizing antibodies, at the concentrations recommended by the manufacturer.

Protein arrays and ELISAs

The protein array kit RayBio® Human Cytokine Antibody Array 5 was purchased from Ray Biotech and performed according to the manufacturer's instructions. See http://www.raybiotech.com/map/human_5_map.pdf for the complete list of 79 factors. ELISAs for human VEGF, HGF and IGF1 (hVEGF, hHGF, hIGF1; R&D Systems) were performed according to the manufacturer's instructions. Concentration values were normalized to the protein content of the lysate of the conditioning cultures, as follows: (concentration of factor) × (total volume of media) / (total protein content of the lysate of the conditioning culture).

NRVM culture and FACS analysis

NRVMs were isolated as described[2] and plated confluent on FN-coated multi-well plates in 10% FBS BM with 19.4mmol/L glucose. Cells were switched to 2% FBS two days after plating. After 4-5 days cells were washed 3 times and media were replaced with CM or FBS-free BM. Plates were incubated in humidified 2% O_2 atmosphere for 24 or 72 hours (fig.1b). Cells were then collected by trypsinization, incubated for 15 minutes at room temperature with Annexin V-FITC and 7AAD (BD Biosciences), and analyzed with a

FACScan flow cytometer and CellQuest software (BD Biosciences). Unlabeled cells were used as a control. Each condition was tested in triplicate on CM from 3 different CDC lines.

Angiogenesis assay

HUVECs were plated on pre-cast, matrix-coated 96-well plates (BD Biosciences), 2×10^4 cells per well. They were plated either with endothelial cell media (ECM; Lonza), as positive control, or with CM (fig.1b), or with FBS-free BM, as the negative control. Cells were imaged after 18 hours with the same settings of zoom, image size and resolution in all experiments. Multiple pictures were taken to cover the entire surface of each well, and then assembled to reconstruct the complete image of every well (Online fig.1). The total tube length was then measured with the ImageJ plug-in, NeuronJ (NIH, http://rsb.info.nih.gov/ij). Each condition was tested in quadruplicate on CM from 3 different CDC lines.

Lentivirus Creation and Cell Transduction

Third generation lentivirus (Lv) was produced by calcium-phosphate co-precipitation transfection of four Lv plasmids (pRRLsin18.cPPT.CMV.Luc.Wpre, pMDLg/p RRE, pMD2.VSV.G, and pRSV-REV) into HEK 293T cells (ATCC) as previously described[3]. Luc encodes for the firefly luciferase gene. The viral supernatant was collected 48 and 72 hours after transfection, filter sterilized using 0.2μm cellulose acetate filter units (Corning) and concentrated by ultra-filtration (100,000 MWCO, Millipore). Transduction titer was assigned on concentrated viral stock three days after transduction by assessing Luc expression in HEK 293T cells transduced in the presence of 8μg/mL of polybrene (Sigma). Transduction efficiencies of greater than 70% were achieved in human CDCs with an MOI of 20 for 24 hours in the presence of 8μg/ml polybrene without impairing normal growth and proliferation.

Mouse myocardial infarction model

SCID beige mice (10 weeks old) were subjected to LAD ligation as previously described[1], and 1×10^5 CDCs or NHDFs were acutely injected into the infarct border zone. Animals were sacrificed 1 day, 1 week or 3 weeks after cell delivery. Regional tissue samples, ranging from 15 to 20 mg on average, were taken from infarct (INF), border zone (BZ), right ventricle (RV) and septum (SEP) areas for WB and RT-PCR analysis (fig.1b). For sectioning, hearts were arrested in diastole by washing them in hyperkalemic solution (30mmol/L KCl, 154mmol/L NaCl), fixed in formalin and paraffin embedded. At least 3 animals per group were considered for each experimental setting.

LVEF was calculated with VisualSonics V1.3.8 software from 2D long-axis views taken through the infarcted area.

Optical Imaging

Mice were given lentivirally-transduced CDCs containing the luciferase gene and then subjected to optical imaging 1 day, 4 days, 1 week, 2 weeks, and 3 weeks post-MI. Mice were anesthetized and injected intraperitoneally with D-luciferin (30mg/kg, GOLD Biotechnology) dissolved in PBS and placed immediately into the IVIS® SPECTRUM (Xenogen) imaging chamber. Images were acquired every 4 minutes with a 1 minute

exposure time until the peak signal was obtained. For visualization purposes, the luminescent image was overlaid on a photographic image. Peak radiance values (signal intensity minus background and corrected for exposure time and angle) was recorded, together with radiance within a region of interest over the anterior chest wall. Data were obtained and analyzed using Living Image® software (Xenogen). The signal obtained on day 1 was used to normalize the signal obtained on subsequent days.

Protein lysate preparation and western blotting

Cell cultures were lysed in lysis buffer (20mmol/L TrisHCl, 5mmol/L EDTA, 50mmol/L NaCl, 1% SDS) with proteinase inhibitors cocktail (Sigma), and homogenized by sonication. Tissue samples were lysed in lysis buffer with proteinase inhibitors cocktail (Roche) and homogenized with a rotor-stator homogenizer. Homogenates were spun at 12,000 rcf for 15 minutes at 4°C. Supernatants were then collected and stored at −80°C, after quantification by Lowry assay of the protein content (BioRad). Lysates were loaded on 4-12% Bis-Tris gels (Invitrogen), and WB on 50μg of protein per lane was performed with the Nupage mini-gels system (Invitrogen). Membranes were blocked in 5% non-fat milk (Biorad) or 5% BSA in TBS 0.05% Tween (TBST; Sigma), and incubated overnight with primary antibodies: hVEGF and pan-GAPDH (Abcam), hHGF and hIGF1 (R&D Systems), hGAPDH (LabFrontier), Akt (Cell Signaling Technology), Caspase 3 (Csp3; Santa Cruz). Human specificity was tested (Online fig.4a). Membranes were washed in TBST, incubated with HRP-conjugated secondary antibodies (Pierce; Santa Cruz), and developed with ECL (Amersham) or West-Femto substrate (Pierce). WB on media was performed with the Nupage system, loading 30μl of media per lane; after blocking, membranes were incubated with HRP-conjugated anti-mouse IgG antibody (Santa Cruz). Densitometric analysis was performed with ImageJ software and plotted as ratios to the GAPDH signal.

RNA extraction and PCR

RNA from cells and tissue samples was extracted with column-based kits (Qiagen). Reverse transcription was performed on 1μg starting RNA (Stratagene) in a 20μl reaction, and 2μl of cDNA product were then subjected to PCR (Invitrogen) with human specific or pan-specific primers for 35 thermal cycles. See Online Table 1 for primer sequences and melting temperatures. PCR products were sequenced to confirm species-specificity, when needed (Online fig.4b).

Immunofluorescence, histology, capillary and TUNEL stainings

CSps and CDCs were fixed for 10 minutes with ethanol-acetone 50:50% at 4°C. Hearts were cut in 8μm sections. After deparaffinization and rehydration of the tissue sections, slides were washed and permeabilized with 0.1% Triton X-100 (Sigma) in PBS with 1% BSA, then blocked in 10% goat serum and incubated overnight at 4°C in 1% goat serum with primary antibodies: anti hVEGF and human nuclear antigen (HNA; Chemicon), hHGF, hIGF1 and CD105 (R&D Systems), FN, KDR and c-kit (Abcam), Met and nkx2.5 (Santa Cruz), IGF1-R (Upstate). Slides were then washed and incubated with Alexa Fluor 488 or 568-conjugated secondary antibodies (Invitrogen). Incubation with secondary antibodies alone did not give any detectable background signal.

For capillary staining, sections were incubated for 2 hours with FITC-conjugated Isolectin B4 (Lab Frontier) and Alexa-568-Phalloidin (Invitrogen); a total of 26700 nuclei were analyzed overall on multiple sections of the border zone, of which 3300 for the assessment of CDC contribution. Co-incubation of isolectin B4 with 500mM galactose was used as a negative control.

TUNEL staining was performed according to the manufacturer's instructions (In situ Cell Death Detection Kit, TMR red, Roche) and quantified on a total of 20500 nuclei in the border zone.

Confocal fluorescence imaging was performed on an Eclipse TE2000-U equipped with a krypton/argon laser using UltraVIEW software (Perkin Elmer). For image analysis of capillary and TUNEL slides, the ImageJ software was used for binary threshold of fluorescent images for each channel and consequent particle count. Masson's Trichrome staining was performed and analyzed as previously described[1]. Briefly, staining was performed according to the kit manufacturer instructions (Sigma). High resolution images were acquired and processed with ImageJ software: color channels were split and the infarct area was manually traced on the blue channel. Threshold adjustment and area measurement functions allowed automatic calculation of the collagen-stained fraction within the defined infarct region.

Supplementary Material

Refer to Web version on PubMed Central for supplementary material.

Acknowledgments

We thank Hunter Champion for obtaining human specimens; Michelle K. Leppo for performing animal surgery; and Mohammed Zauher and Andreas S. Barth for assistance with cell culture.

Sources of Funding

This work was supported by the National Heart, Lung, and Blood Institute; NIH; and Donald W. Reynolds Foundation (to E. Marbán).

Non-standard Abbreviations and Acronyms

BM	basal media
BZ	border zone
CDC	cardiosphere-derived cell
CM	conditioned media
CSp	cardiosphere
GF	growth factor
HGF	hepatocyte growth factor
HNA	human nuclear antigen

HUVEC	human umbilical vein endothelial cell
IGF	insulin-like growth factor
IICSp	secondary cardiosphere
LVEF	left ventricular ejection fraction
MHC	myosin heavy chain
MI	myocardial infarction
NHDF	normal human dermal fibroblast
NRVM	neonatal rat ventricular myocyte
VEGF	vascular endothelial growth factor
WB	Western blot

References

1. Rosenzweig A. Cardiac cell therapy-mixed results from mixed cells. *N Engl J Med*.. 2006; 355:1274–1277. [PubMed: 16990391]
2. Smith RR, Barile L, Messina E, Marban E. Stem cells in the heart: what's the buzz all about? Part 1: preclinical considerations. *Heart Rhythm*.. 2008; 5:749–757. [PubMed: 18452881]
3. Smith RR, Barile L, Messina E, Marban E. Stem cells in the heart: what's the buzz all about? Part 2: arrhythmic risks and clinical studies. *Heart Rhythm*.. 2008; 5:880–887. [PubMed: 18534373]
4. Dimmeler S, Burchfield J, Zeiher AM. Cell-based therapy of myocardial infarction. *Arterioscler Thromb Vasc Biol*.. 2008; 28:208–216. [PubMed: 17951319]
5. Guan K, Hasenfuss G. Do stem cells in the heart truly differentiate into cardiomyocytes? *J Mol Cell Cardiol*.. 2007; 43:377–387. [PubMed: 17716688]
6. Welt FG, Losordo DW. Cell therapy for acute myocardial infarction: curb your enthusiasm? Circulation. 2006; 113:1272–1274. [PubMed: 16534025]
7. Cho HJ, Lee N, Lee JY, Choi YJ, Ii M, Wecker A, Jeong JO, Curry C, Qin G, Yoon YS. Role of host tissues for sustained humoral effects after endothelial progenitor cell transplantation into the ischemic heart. *J Exp Med*.. 2007; 204:3257–3269. [PubMed: 18070934]
8. Ebelt H, Jungblut M, Zhang Y, Kubin T, Kostin S, Technau A, Oustanina S, Niebrugge S, Lehmann J, Werdan K, Braun T. Cellular cardiomyoplasty: improvement of left ventricular function correlates with the release of cardioactive cytokines. Stem Cells. 2007; 25:236–244. [PubMed: 16973829]
9. Gnecchi M, He H, Noiseux N, Liang OD, Zhang L, Morello F, Mu H, Melo LG, Pratt RE, Ingwall JS, Dzau VJ. Evidence supporting paracrine hypothesis for Akt-modified mesenchymal stem cell-mediated cardiac protection and functional improvement. *FASEB J*.. 2006; 20:661–669. [PubMed: 16581974]
10. Kinnaird T, Stabile E, Burnett MS, Lee CW, Barr S, Fuchs S, Epstein SE. Marrow-derived stromal cells express genes encoding a broad spectrum of arteriogenic cytokines and promote in vitro and in vivo arteriogenesis through paracrine mechanisms. *Circ Res*.. 2004; 94:678–685. [PubMed: 14739163]
11. Gnecchi M, He H, Liang OD, Melo LG, Morello F, Mu H, Noiseux N, Zhang L, Pratt RE, Ingwall JS, Dzau VJ. Paracrine action accounts for marked protection of ischemic heart by Akt-modified mesenchymal stem cells. *Nat Med*.. 2005; 11:367–368. [PubMed: 15812508]
12. Gnecchi M, Zhang Z, Ni A, Dzau VJ. Paracrine mechanisms in adult stem cell signaling and therapy. *Circ Res*.. 2008; 103:1204–1219. [PubMed: 19028920]

13. Messina E, De Angelis L, Frati G, Morrone S, Chimenti S, Fiordaliso F, Salio M, Battaglia M, Latronico MV, Coletta M, Vivarelli E, Frati L, Cossu G, Giacomello A. Isolation and expansion of adult cardiac stem cells from human and murine heart. *Circ Res*.. 2004; 95:911–921. [PubMed: 15472116]

14. Smith RR, Barile L, Cho HC, Leppo MK, Hare JM, Messina E, Giacomello A, Abraham MR, Marban E. Regenerative potential of cardiosphere-derived cells expanded from percutaneous endomyocardial biopsy specimens. Circulation. 2007; 115:896–908. [PubMed: 17283259]

15. Davis DR, Zhang Y, Smith RR, Cheng K, Terrovitis J, Malliaras K, Li TS, White A, Makkar R, Marbán E. Validation of the cardiosphere method to culture cardiac progenitor cells from myocardial tissue. PLoS ONE. 2009; 4:e7195. [PubMed: 19779618]

16. Tang YL, Zhu W, Cheng M, Chen L, Zhang J, Sun T, Kishore R, Phillips MI, Losordo DW, Qin G. Hypoxic preconditioning enhances the benefit of cardiac progenitor cell therapy for treatment of myocardial infarction by inducing CXCR4 expression. *Circ Res*.. 2009; 104:1209–1216. [PubMed: 19407239]

17. Takehara N, Tsutsumi Y, Tateishi K, Ogata T, Tanaka H, Ueyama T, Takahashi T, Takamatsu T, Fukushima M, Komeda M, Yamagishi M, Yaku H, Tabata Y, Matsubara H, Oh H. Controlled delivery of basic fibroblast growth factor promotes human cardiosphere-derived cell engraftment to enhance cardiac repair for chronic myocardial infarction. *J Am Coll Cardiol*.. 2008; 52:1858–1865. [PubMed: 19038683]

18. Hausenloy DJ, Yellon DM. Cardioprotective growth factors. *Cardiovasc Res*.. 2009; 83:179–194. [PubMed: 19218286]

19. Davis ME, Hsieh PC, Takahashi T, Song Q, Zhang S, Kamm RD, Grodzinsky AJ, Anversa P, Lee RT. Local myocardial insulin-like growth factor 1 (IGF-1) delivery with biotinylated peptide nanofibers improves cell therapy for myocardial infarction. Proc Natl Acad Sci U S A. 2006; 103:8155–8160. [PubMed: 16698918]

20. Jin H, Wyss JM, Yang R, Schwall R. The therapeutic potential of hepatocyte growth factor for myocardial infarction and heart failure. *Curr Pharm Des*.. 2004; 10:2525–2533. [PubMed: 15320761]

21. Ueda H, Nakamura T, Matsumoto K, Sawa Y, Matsuda H, Nakamura T. A potential cardioprotective role of hepatocyte growth factor in myocardial infarction in rats. *Cardiovasc Res*.. 2001; 51:41–50. [PubMed: 11399246]

22. Li Q, Li B, Wang X, Leri A, Jana KP, Liu Y, Kajstura J, Baserga R, Anversa P. Overexpression of insulin-like growth factor-1 in mice protects from myocyte death after infarction, attenuating ventricular dilation, wall stress, and cardiac hypertrophy. *J Clin Invest*.. 1997; 100:1991–1999. [PubMed: 9329962]

23. Banai S, Shweiki D, Pinson A, Chandra M, Lazarovici G, Keshet E. Upregulation of vascular endothelial growth factor expression induced by myocardial ischaemia: implications for coronary angiogenesis. *Cardiovasc Res*.. 1994; 28:1176–1179. [PubMed: 7525061]

24. Luo Z, Diaco M, Murohara T, Ferrara N, Isner JM, Symes JF. Vascular endothelial growth factor attenuates myocardial ischemia-reperfusion injury. *Ann Thorac Surg*.. 1997; 64:993–998. [PubMed: 9354516]

25. Ferrarini M, Arsic N, Recchia FA, Zentilin L, Zacchigna S, Xu X, Linke A, Giacca M, Hintze TH. Adeno-associated virus-mediated transduction of VEGF165 improves cardiac tissue viability and functional recovery after permanent coronary occlusion in conscious dogs. *Circ Res*.. 2006; 98:954–961. [PubMed: 16543500]

26. Guo Y, He J, Wu J, Yang L, Dai S, Tan X, Liang L. Locally overexpressing hepatocyte growth factor prevents post-ischemic heart failure by inhibition of apoptosis via calcineurin-mediated pathway and angiogenesis. *Arch Med Res*.. 2008; 39:179–188. [PubMed: 18164961]

27. Tse HF, Siu CW, Zhu SG, Songyan L, Zhang QY, Lai WH, Kwong YL, Nicholls J, Lau CP. Paracrine effects of direct intramyocardial implantation of bone marrow derived cells to enhance neovascularization in chronic ischaemic myocardium. Eur J Heart Fail. 2007; 9:747–753. [PubMed: 17481945]

28. Uemura R, Xu M, Ahmad N, Ashraf M. Bone marrow stem cells prevent left ventricular remodeling of ischemic heart through paracrine signaling. Circ Res. 2006; 98:1414–1421. [PubMed: 16690882]

29. Urbanek K, Rota M, Cascapera S, Bearzi C, Nascimbene A, De Angelis A, Hosoda T, Chimenti S, Baker M, Limana F, Nurzynska D, Torella D, Rotatori F, Rastaldo R, Musso E, Quaini F, Leri A, Kajstura J, Anversa P. Cardiac stem cells possess growth factor-receptor systems that after activation regenerate the infarcted myocardium, improving ventricular function and long-term survival. Circ Res. 2005; 97:663–673. [PubMed: 16141414]

30. Kim SJ, Abdellatif M, Koul S, Crystal GJ. Chronic treatment with insulin-like growth factor-1 enhances myocyte contraction by upregulation of Akt-SERCA2a signaling pathway. Am J Physiol Heart Circ Physiol. 2008; 295:H130–H135. [PubMed: 18456736]

31. Iravanian S, Nabutovsky Y, Kong CR, Saha S, Bursac N, Tung L. Functional reentry in cultured monolayers of neonatal rat cardiac cells. Am J Physiol Heart Circ Physiol. 2003; 285:H449–H456. [PubMed: 12623789]

32. Li Z, Lee A, Huang M, Chun H, Chung J, Chu P, Hoyt G, Yang P, Rosenberg J, Robbins RC, Wu JC. Imaging survival and function of transplanted cardiac resident stem cells. J Am Coll Cardiol. 2009; 53:1229–1240. [PubMed: 19341866]

33. Terrovitis J, Kwok KF, Lautamaki R, Engles JM, Barth AS, Kizana E, Miake J, Leppo MK, Fox J, Seidel J, Pomper M, Wahl RL, Tsui B, Bengel F, Marban E, Abraham MR. Ectopic expression of the sodium-iodide symporter enables imaging of transplanted cardiac stem cells in vivo by single-photon emission computed tomography or positron emission tomography. J Am Coll Cardiol. 2008; 52:1652–1660. [PubMed: 18992656]

34. Krishnan M, Park JM, Cao F, Wang D, Paulmurugan R, Tseng JR, Gonzalgo ML, Gambhir SS, Wu JC. Effects of epigenetic modulation on reporter gene expression: implications for stem cell imaging. FASEB J. 2006; 20:106–108. [PubMed: 16246867]

35. Kelm JM, Ehler E, Nielsen LK, Schlatter S, Perriard JC, Fussenegger M. Design of artificial myocardial microtissues. Tissue Eng. 2004; 10:201–214. [PubMed: 15009946]

36. Al-Moundhri MS, Al-Shukaili A, Al-Nabhani M, Al-Bahrani B, Burney IA, Rizivi A, Ganguly SS. Measurement of circulating levels of VEGF-A, -C, and -D and their receptors, VEGFR-1 and -2 in gastric adenocarcinoma. World J Gastroenterol. 2008; 14:3879–3883. [PubMed: 18609713]

37. Taniguchi T, Kitamura M, Arai K, Iwasaki Y, Yamamoto Y, Igari A, Toi M. Increase in the circulating level of hepatocyte growth factor in gastric cancer patients. Br J Cancer. 1997; 75:673–677. [PubMed: 9043023]

38. Yakar S, Rosen CJ, Beamer WG, Ackert-Bicknell CL, Wu Y, Liu JL, Ooi GT, Setser J, Frystyk J, Boisclair YR, LeRoith D. Circulating levels of IGF-1 directly regulate bone growth and density. J Clin Invest. 2002; 110:771–781. [PubMed: 12235108]

39. Johnston PV, Sasano T, Mills K, Evers R, Lee ST, Smith RR, Lardo AC, Lai S, Steenbergen C, Gerstenblith G, Lange R, Marban E. Engraftment, differentiation, and functional benefits of autologous cardiosphere-derived cells in porcine ischemic cardiomyopathy. Circulation. 2009; 120:1075–1083. [PubMed: 19738142]

40. Rota M, Padin-Iruegas ME, Misao Y, De Angelis A, Maestroni S, Ferreira-Martins J, Fiumana E, Rastaldo R, Arcarese ML, Mitchell TS, Boni A, Bolli R, Urbanek K, Hosoda T, Anversa P, Leri A, Kajstura J. Local activation or implantation of cardiac progenitor cells rescues scarred infarcted myocardium improving cardiac function. Circ Res. 2008; 103:107–116. [PubMed: 18556576]

41. Isner JM. Myocardial gene therapy. Nature. 2002; 415:234–239. [PubMed: 11805848]

42. Laham RJ, Simons M, Sellke F. Gene transfer for angiogenesis in coronary artery disease. Annu Rev Med. 2001; 52:485–502. [PubMed: 11160791]

43. Lei Y, Haider H, Shujia J, Sim ES. Therapeutic angiogenesis. Devising new strategies based on past experiences. Basic Res Cardiol. 2004; 99:121–132. [PubMed: 14963670]

ONLINE SUPPLEMENTAL REFERENCES

1. Smith RR, Barile L, Cho HC, Leppo MK, Hare JM, Messina E, Giacomello A, Abraham MR, Marban E. Regenerative potential of cardiosphere-derived cells expanded from percutaneous endomyocardial biopsy specimens. Circulation. 2007; 115:896–908. [PubMed: 17283259]

2. Iravanian S, Nabutovsky Y, Kong CR, Saha S, Bursac N, Tung L. Functional reentry in cultured monolayers of neonatal rat cardiac cells. Am J Physiol Heart Circ Physiol. 2003; 285:H449–456. [PubMed: 12623789]

3. Kizana E, Ginn SL, Allen DG, Ross DL, Alexander IE. Fibroblasts can be genetically modified to produce excitable cells capable of electrical coupling. Circulation. 2005; 111:394–398. [PubMed: 15687125]

4. Zhang YW, Su Y, Lanning N, Gustafson M, Shinomiya N, Zhao P, Cao B, Tsarfaty G, Wang LM, Hay R, Vande Woude GF. Enhanced growth of human met-expressing xenografts in a new strain of immunocompromised mice transgenic for human hepatocyte growth factor/scatter factor. Oncogene. 2005; 24:101–106. [PubMed: 15531925]

5. Zeng F, Chen MJ, Baldwin DA, Gong ZJ, Yan JB, Qian H, Wang J, Jiang X, Ren ZR, Sun D, Huang SZ. Multiorgan engraftment and differentiation of human cord blood CD34+ Lin-cells in goats assessed by gene expression profiling. Proc atl Acad Sci U S A. 2006; 103:7801–7806.

6. Choi SJ, Oba Y, Gazitt Y, Alsina M, Cruz J, Anderson J, Roodman GD. Antisense inhibition of macrophage inflammatory protein 1-alpha blocks bone destruction in a model of myeloma bone disease. J Clin Invest. 2001; 108:1833–1841. [PubMed: 11748267]

Novelty and Significance

What Is Known?

- Cardiac cell therapy for heart failure represents a major opportunity in regenerative medicine, and multiple stem cell populations are currently being evaluated as therapeutic tools, both in preclinical and clinical models.
- Various lines of evidence indicate that direct differentiation of transplanted cells in cardiac tissue is not the only mechanism underlying the observed beneficial outcomes in animal models and early clinical trials.
- CDCs are a resident progenitor population currently in clinical trials; they are easily harvested from percutaneous endomyocardial biopsies, can directly differentiate into multiple lineages when injected into the heart, and they are effective in mouse and pig models of heart failure therapy.

What New Information Does This Article Contribute?

- Human cardiospheres and CDCs are able to secrete a wide variety of humoral factors, and their conditioned media exerts prosurvival and angiogenic biological effects on cell cultures of cardiomyocytes and endothelial cells.
- In a mouse model of myocardial infarction, human CDCs release growth factors in the tissue, reduce apoptosis, and increase both viability and perfusion in heart tissue.
- The direct contribution of injected CDCs to cardiac tissue represents approximately 20% to 50% of the overall increase in capillary and cardiomyocyte densities and tissue viability; accordingly, indirect effects on tissue preservation and/or recruitment of endogenous regeneration significantly contribute to the therapeutic outcome.

We investigated the mechanisms underlying the functional benefit of transplanted cardiosphere-derived cells (CDCs) in the injured heart. Our results show that CDCs have a wide and potent paracrine potential, exerting antiapoptotic and proangiogenic effects in vitro, while improving tissue viability and function in vivo. Quantification of the relative contributions of direct versus indirect mechanisms revealed a major role for CDC-mediated humoral effects on parenchymal preservation and endogenous repair. Although direct differentiation occurs, it accounts for only 20% to 50% of the overall increases in capillary and cardiomyocyte density. The findings stress the importance of early paracrine effects in the mechanism of benefit, even with endogenous cardiac cells that can unambiguously regenerate the heart directly.

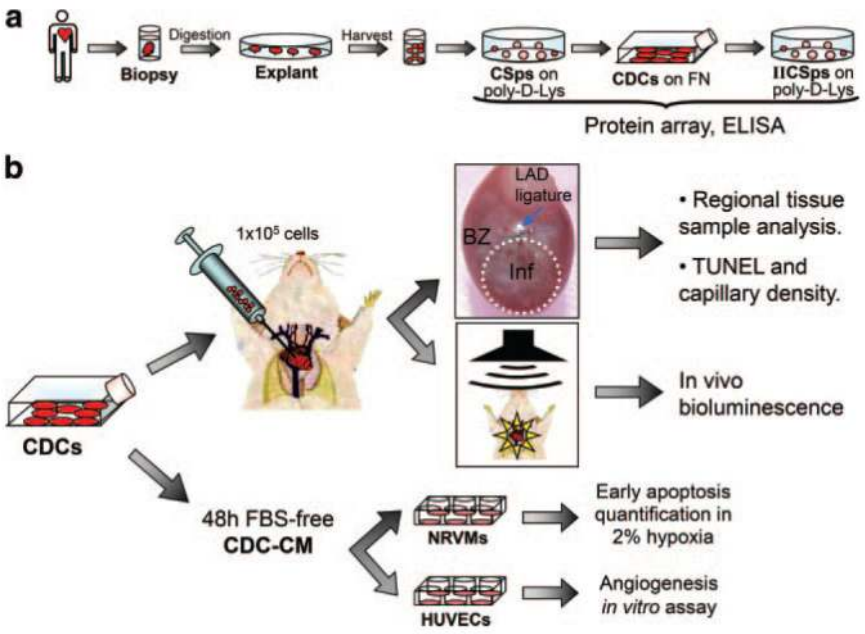

Figure 1. Experimental design

a, Culture protocol for CSps, CDCs, and IICSps isolation. **b,** Two sets of functional experiments were based on CDCs: in vivo injection of 1×10^5 cells in a SCID mouse MI model for regional tissue samples analysis, histology, and luciferase detection; and in vitro assessment of CDC-CM effects on NRVM viability or HUVEC angiogenic abilities. CMs were collected after 48 hours from CDCs (or NHDFs as control) and used to plate NRVMs in 2% hypoxia or HUVECs on matrix-coated wells.

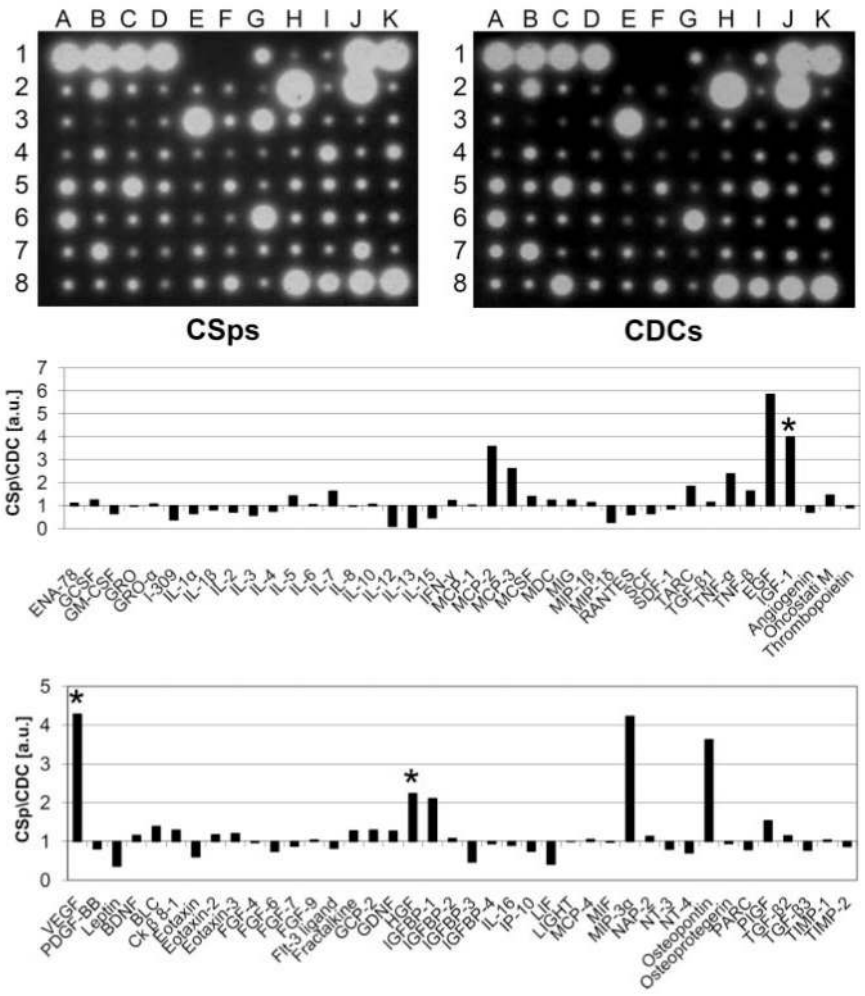

Figure 2. Cytokines and growth factors in vitro screening

Representative images of protein arrays on serum-free CM from CSps and CDCs, as well as corresponding densitograms of the CSp/CDC levels ratios for each spot. *Three selected factors of interest.

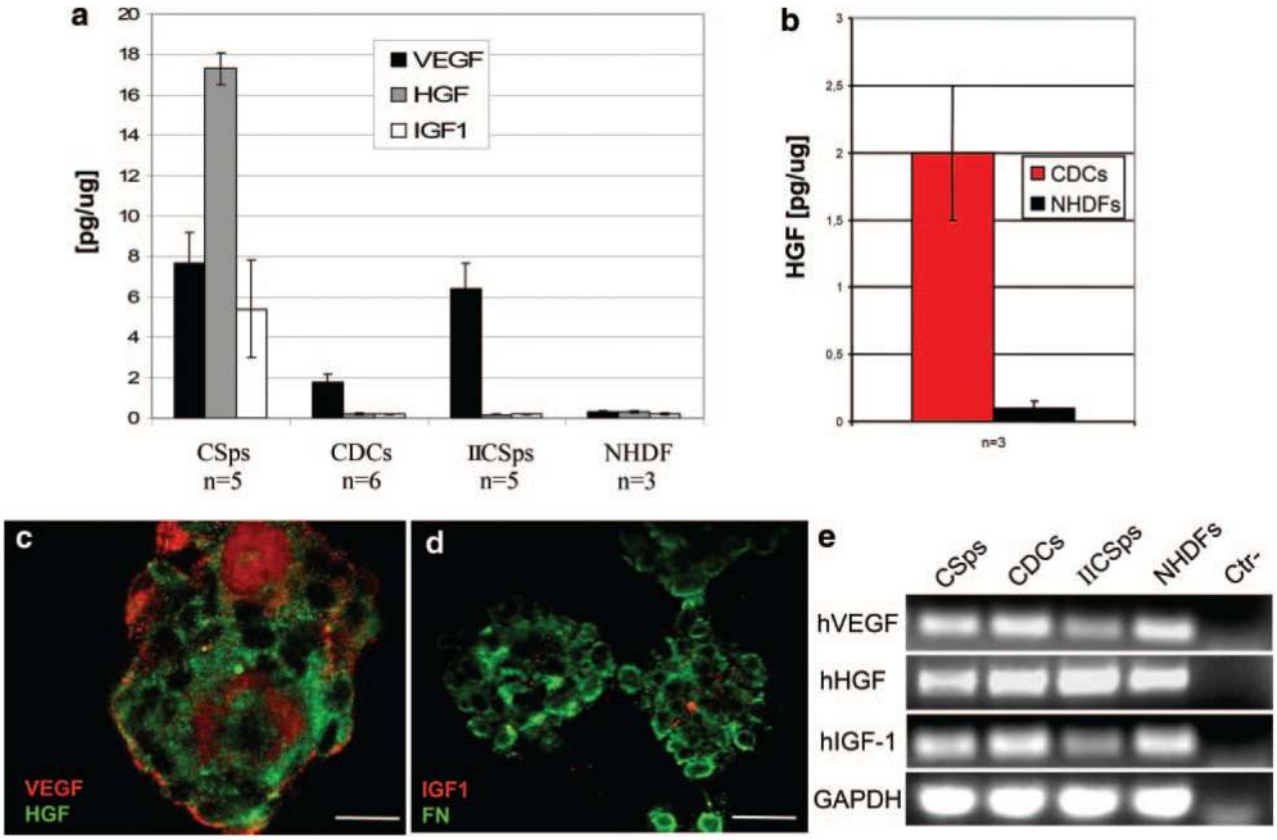

Figure 3. VEGF, HGF, and IGF1 secretion levels in vitro

CSps secrete VEGF, HGF, and IGF1 in vitro in low serum media, whereas in the same conditions, CDCs and IICSps only secrete VEGF **(a)**. HGF release by CDCs is recovered in serum-free BM **(b)**. Confocal images of CSps stained for VEGF and HGF **(c)** and IGF1 and fibronectin (FN) **(d)** allowed GF detection in their 3D structure. RT-PCR for GFs in CSps, CDCs, IICSps, and NHDFs is shown in **e**. **Scale bars**=100 μm.

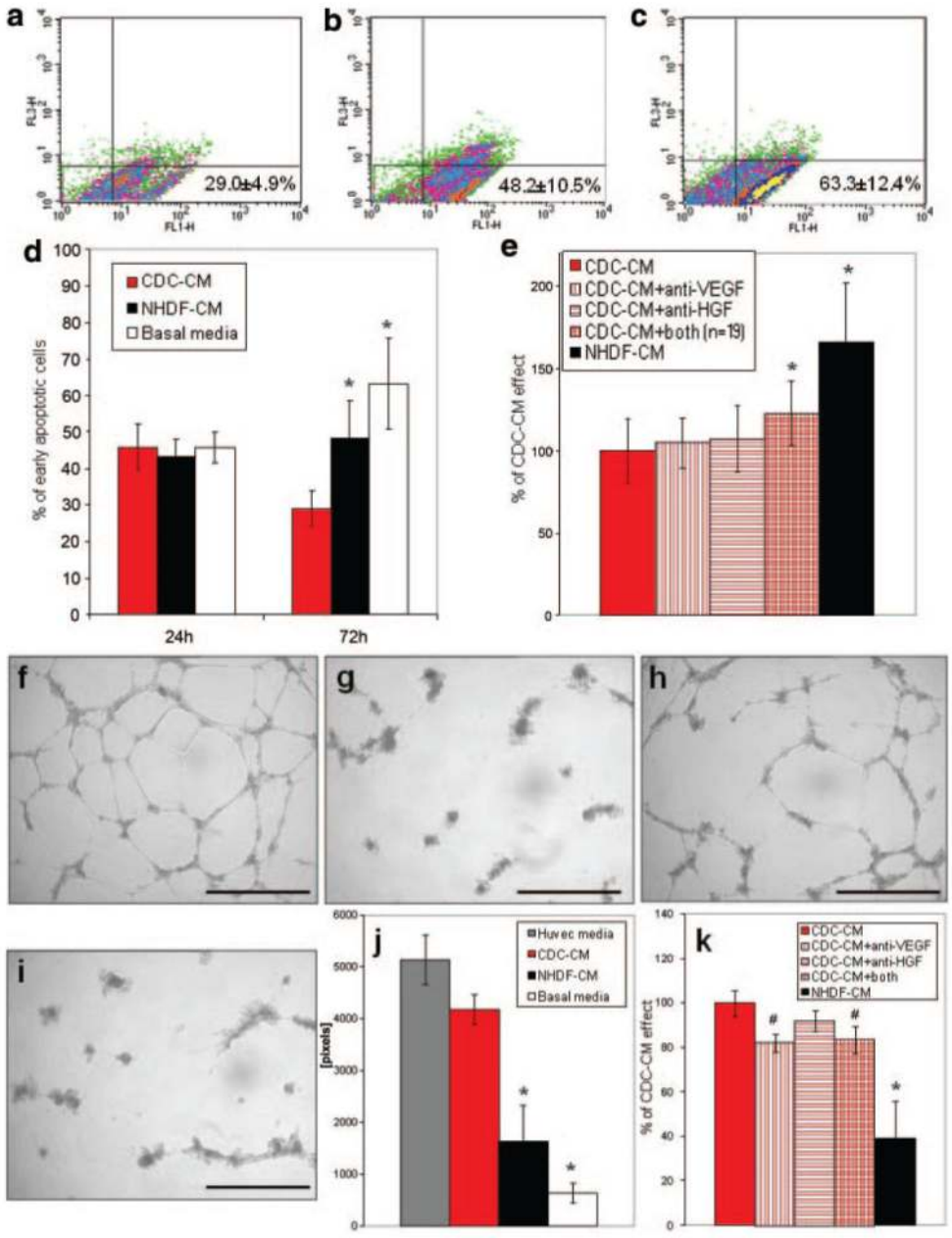

Figure 4. Prosurvival and proangiogenic in vitro effects of CDC-CM

NRVMs were plated with CM in 2% hypoxia up to 72 hours. **a through c,** Representative density plots of early apoptotic NRVMs cultured for 72 hours in CDC-CM (n=11), NHDF-CM (n=11), or BM (n=7), respectively. Average percentages of 7AAD^{-}/Annexin V^{+} (FL1-H and FL3-H, respectively) are shown at the **lower right** of each **graph**. Data are summarized in **graph d** (n=5 per group at 24 hours). **e,** Preincubation of CDC-CM with VEGF and HGF neutralizing antibodies (n=19) significantly reduced viable NRVMs after 72 hours. **f through i,** Representative images of HUVECs 18 hours after plating on matrix-coated wells in endothelial cell media **(f)**, serum-free BM **(g)**, CMC-CM **(h)**, and NHDF-CM **(i)**. **j,** Quantification of total tube length in the different media. Preincubation of CDC-

CM with VEGF neutralizing antibody significantly reduced the positive effect **(k)**. *P<0.001, #P<0.05 vs CDC group. **Scale bars**=1 mm.

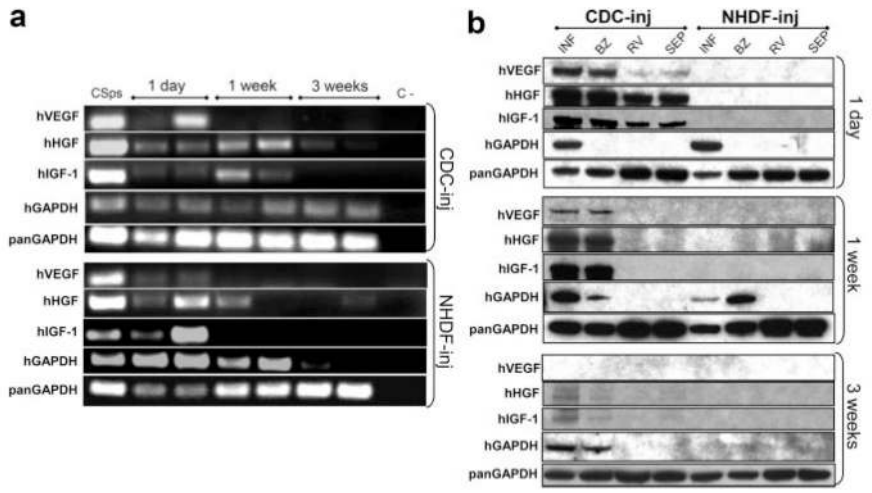

Figure 5. Human GFs are detectable in infarcted CDC-injected hearts

Human mRNAs for VEGF, HGF, and IGF1 are detectable in the infarcted tissue from murine hearts up to 3 weeks after LAD ligation and cell delivery, both in CDC- and NHDF-injected mice **(a)**. For each time point, PCR products from 2 different animals are shown. Human VEGF, HGF, and IGF1 proteins are detectable with human specific antibodies in CDC-injected hearts at different time points, but not in NHDF-injected **(b)**, although human GAPDH detection confirms engraftment in both groups. Inj indicates injected; INF, infarct; BZ, border zone; RV, right ventricle; SEP, septum.

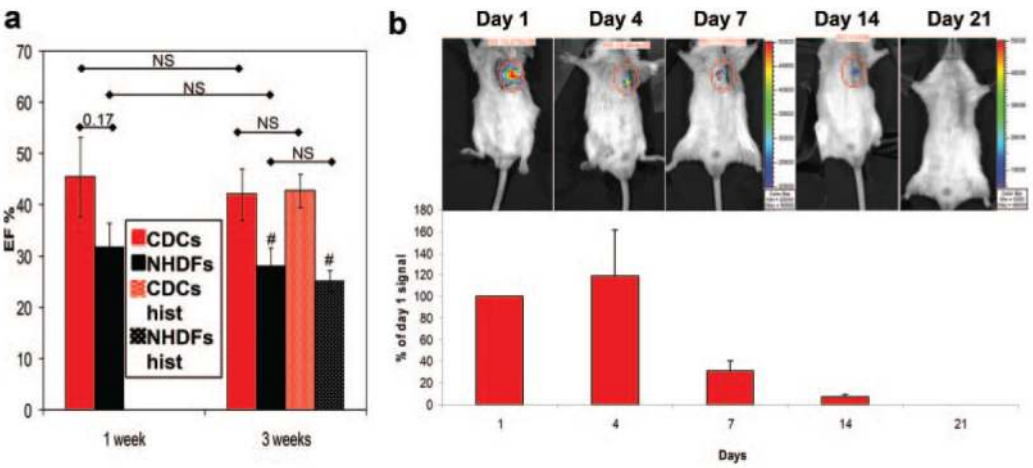

Figure 6. Functional and engraftment evaluation in vivo

a, Comparison of LVEF in mice groups from the present study to 2 historical groups (hist) from a previous study.[14] Data are plotted as averages±SEM. #$P<0.05$ vs the corresponding CDC group. NS: not statistically significant. **b:** Engraftment follow-up by in vivo bioluminescence on luciferase-labeled CDC injected mice. Signal intensity is normalized to that of day 1. Note that the representative images at 14 and 21 days have an expanded color scale bar.

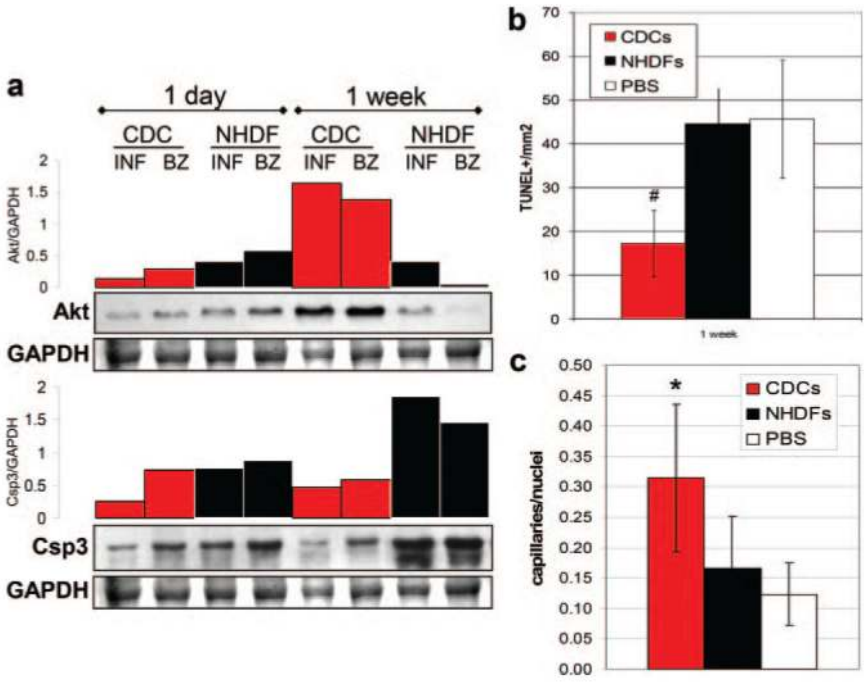

Figure 7. Tissue viability and perfusion assessment at molecular and histological levels

a, WB for Akt and corresponding densitometric plots, normalized to GAPDH, showed that 1 week after surgery Akt expression was higher in infarct (INF) and BZ tissue from CDC-injected compared to NHDF-injected mice. Consistently, at the same time point, Csp3 protein levels were lower in CDC-injected hearts. **b and c,** Quantification of the TUNEL-positive cell density **(b)** and capillary density **(c)** in the BZ of infarcted mice 1 week after cell delivery. **P*<0.001 and #*P*<0.05 vs control groups.

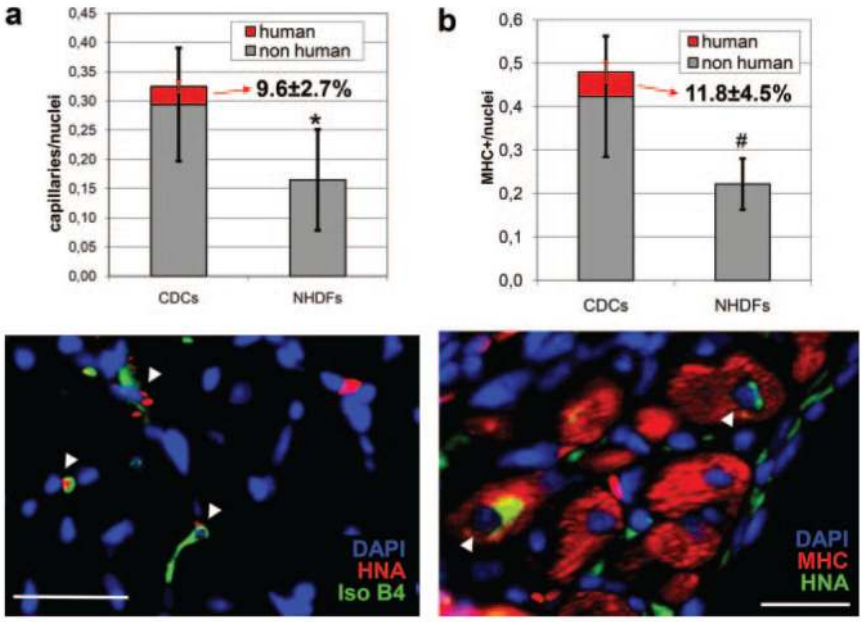

Figure 8. Human contribution to capillaries and MHC-positive cells in engraftment areas

a, Double staining for isolectin-B4 and HNA allowed assessment of CDC contribution to the overall capillary density in engrafted areas in the border zone. **b,** Double staining for MHC and HNA allowed quantification of direct muscle regeneration in the viable tissue areas of the infarct. **P*<0.001 and #*P*<0.05 vs CDC group (in **graph a** refers to both overall counts and nonhuman only counts). **Scale bars**=25 μm. **Arrowheads** indicate double-positive cells.